Semi-linear description of beam nonlinear propagation

W. NASALSKI

Institute of Fundamental Technological Research, Polish Academy of Sciences, ul. Świętokrzyska 21, 00−049 Warszawa, Poland.

It has recently been shown [1] that propagation in nonlinear Kerr media and propagation in linear media can be consistently interrelated by a transformation that scales a propagation distance, a radius of a phase front curvature and an on-axis beam phase. The transformation is valid for cases of arbitrary transverse dimension of the beam and for power levels up to a self-trapped propagation level. Although the analysis leads to an efficient tracing of the beam by complex rays or nonlinear *ABCD* matrices, an equivalent semi-linear description of nonlinear propagation in terms of four aberration nonlinear effects is possible as well. These effects, *i.e.*, an optical distance self-shortening, a beam waist shift, a beam waist width modification and an on-axis phase shift are introduced and discussed in this paper. A generalization of the method into higher-order mode propagation is also outlined.

1. Introduction

The well-known paraxial aberrationless approximation [2]−[5] is commonly employed in analysis of linear optical systems. The paraxial approximation is usually implemented within a framework of the first-order optics, in which the complex ray or *ABCD* transfer matrix formalisms [3], [4] trace the propagation process. In this approach, field and medium changes up to the second order in transverse coordinates are retained [2], [3], [5] and a space-time analogy [5] allows one to treat beam propagation and pulse propagation through an optical system on the entirely equal footing. On the other hand, in nonlinear optics, a classical theory of self-focusing [7] is also based on the paraxial-ray description of the propagation process. The paraxial aberrationless approximation [8] of a field distribution is used in a common Gaussian self-similar form. This approach actually links the nonlinear process to the linear one through parabolic approximations of transverse field intensity and medium refractive index distributions. Several versions of the paraxial aberrationless analysis have recently been proposed [4], [9]−[17] to simplify the treatment of an optical propagation in nonlinear media. Various nonlinear phenomena have been analyzed in this manner, from the Z-scan measurements [18], [19] of the nonlinear medium parameters or the femtosecond techniques of pulse compression [20]−[22] to the nonspecular interaction of laser beams with linear and nonlinear interfaces [5], [23].

Recently, the paraxial aberrationless method has been refined and generalized into the multidimensional the Scaled Complex Ray Tracing (SCRT) method [1].

The SCRT method approximates a nonlinear Shrödinger equation (NLSE), for the propagation in a nonlinear Kerr medium, by a set of ordinary differential equations for beam parameters of the self-similar Gaussian solution to the nonlinear propagation problem. This set of equations is subsequently transposed by an appropriate scale transformation to a new set of equations, which are characteristic of the linear propagation. In this way the nonlinear process can be traced analytically on the scaled linear level by use of all the well-assessed analytical tools of the linear first order optics [3], [4]. The method is quite general since a full range of excitation power can be considered, from low up to the self-trapped propagation levels in arbitrary dimensions transverse to the propagation direction, and arbitrary propagation ranges including those containing self-collapse points.

From three equivalent modes of SCRT analysis of the nonlinear propagation [1], that is the linear tracing on the scaled linear level, the semi-linear description of the beam field in terms of nonlinear aberrationless effects and the nonlinear tracing by use of the *ABCD* nonlinear matrices, the first two are discussed in this paper. Basic facts on the complex ray tracing are summarized in Section 2, and nonlinear evolution equations of beam parameters, together with their solutions, are given in Section 3. Section 4 is devoted to definitions of the aberrationless nonlinear effects and a generalization of the approach into a higher-order mode nonlinear propagation is outlined in Section 5. Some numerical examples of the aberrationless analysis are also presented. An interpretation of the results is given in the context of the optical beam propagation, although a generalization into a pulse propagation case seems to be straightforward [6].

The aberrationless effects are understood as the nonlinear changes of the beam propagation parameters with respect to the low power, *i.e.*, linear, propagation. The nonlinear fundamental mode propagation can be completely described in terms of four independent aberrationless effects, namely: a self- shortening of the optical path, a waist shift of the beam, a beam waist radius modification and an on-axis beam phase shift. Other nonlinear effects, such as nonlinear changes of a beam on-axis amplitude or a phase front radius of curvature of the beam can be evaluated by use of these four independent effects. The aberrationless effects provide a solution to the problem and a straightforward geometrical interpretation of the nonlinear process. Although the existence of the aberrationless effects has been previously indicated [10], [15], [17], [22], no self- consistent description of the nonlinear propagation in terms of these effects has, to the author's knowledge, been reported so far. The main objective of this contribution is to introduce a complete set of aberrationless effects as an efficient tool of tracing the nonlinear propagation.

2. Nonlinear complex ray tracing of the beam

Let us consider a transversally symmetric Gaussian beam incident upon the nonlinear sample. The low power z and high power ζ propagation distances of the low power and nonlinear propagation are measured from respective beam waist

positions at $z = 0$ and $\zeta = 0$. Each increment of z and ζ represent increments of the propagation distances along the beam axis divided by a low power (linear) refractive index n_L. In paper [1], parameters of the beam have been analyzed with respect to the longitudinal low power coordinate z. However, in order to obtain more straightforward interpretation of a solution, it seems more appropriate to consider the nonlinear propagation with respect to the actual nonlinear optical distance coordinate ζ, instead of z. To get deeper insight into the geometry of the beam field, it is assumed at the beginning, and on the grounds of the results of previous analyses [1], that the linear and nonlinear distances are linearly interrelated according to

$$\zeta - \zeta_0 = \varkappa(z - z_0). \tag{1}$$

By definition, both coordinates z and ζ are equal to each other at some specified (input) plane $z = z_0$ or $\zeta = \zeta_0$, i.e., $z_0 = \zeta_0$, and $\varkappa$ stands for the nonlinear self-shortening factor. The factor $\varkappa$ is one from four independent aberrationless nonlinear effects, all of which are to be given in Sect. 4.
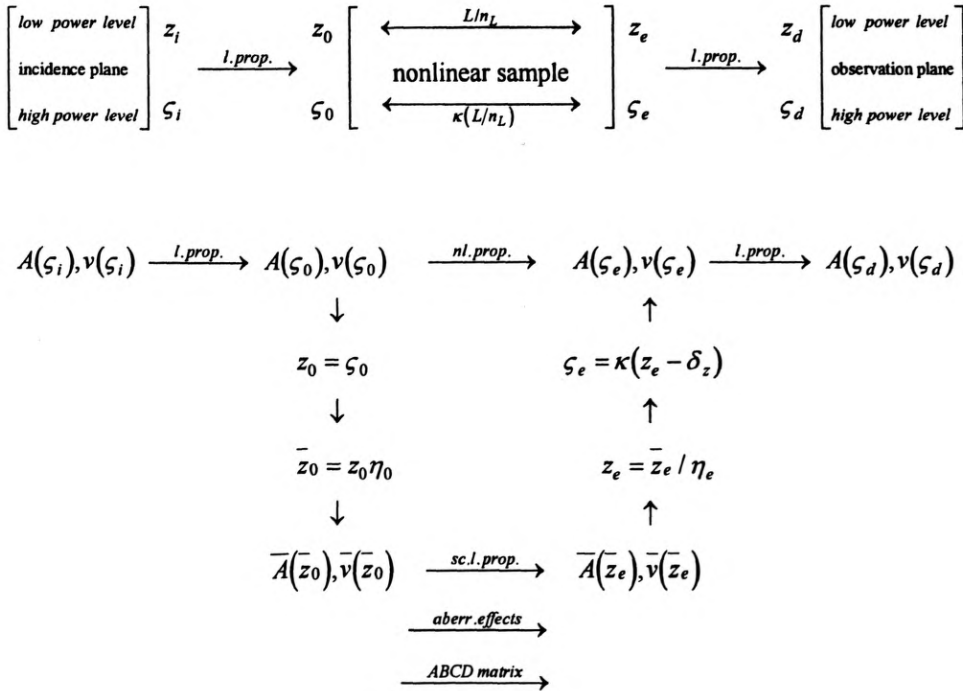

Fig. 1. Schematic of the beam-sample configuration (high level) and the complex ray tracing of the nonlinear propagation (low level): L — sample thickness, n_L — low power refractive index, $\varkappa$ — self-shortening factor, z — low power optical path, ζ — high power optical path, subscripts i, 0, e and d indicate incident, input (front face of the nonlinear sample), output (rear face of the nonlinear sample) and observation planes, respectively. The observation plane can be placed at arbitrary transverse plane $z = \text{const} > z_0$

The geometry of the problem and its solution scheme is sketched in Fig. 1. The incident transversally symmetric beam is defined at arbitrary incident plane at $z = z_i$ or $\zeta = \zeta_i$. The incident beam enters the nonlinear sample at its front (input) face $z = z_0$ or $\zeta = \zeta_0$ and exits it at its rear (output) face at $z = z_e$ or $\zeta = \zeta_e$. An observation plane usually coincides with the rear face of the sample or is chosen far apart from the sample at $z = z_d$ or $\zeta = \zeta_d$, where a diaphragm is placed to convert phase changes, accumulated during the propagation in the sample, into field intensity changes at this plane. However, the observation plane can also be placed inside the nonlinear sample.

At the front face of the nonlinear sample a field distribution is specified by its on-axis amplitude a_0, on-axis phase φ_0, beam radius w_0 and phase front curvature radius R_0. The optical distances z and ζ, as well as the phase curvature radius R, are normalized [23], [1] to the diffraction length $z_D = \beta w_{wL}^2$ ($z \equiv z/z_D$), where β and w_{wL} are a wave number and a waist width radius of the low power beam in the sample, respectively. Moreover, x-coordinates, transverse to the propagation direction along z, and the beam radius w are normalized to w_{wL} ($\underline{x} \equiv \underline{x}/w_{wL}$ and $w \equiv w/w_{wL}$), which also implies $w_0 = (1 + \zeta_0^2)^{1/2}$ and $R_0 = w_0^2/\zeta_0$ [23], [1]. The problem is multidimensional in general, so $\underline{x} \equiv (x_1, \ldots, x_d)$ is a vector of transverse coordinates and d is a number of transverse to z axis dimensions. Note that through this paper the subscript L indicates quantities related to the low power (linear) propagation, and the subscripts 0 and e refer to the quantities evaluated at the input and output planes at $z = z_0$ and $z = z_e$, respectively.

The SCRT description of the nonlinear propagation is based on the common assumption of the self-similar Gaussian shape of the beam and the parabolic approximation of the nonlinear refractive index of the Kerr medium [1]. Therefore, let us postulate that the fundamental transversely symmetric Gaussian beam

$$V(\underline{x}, \zeta) = A(\zeta) \exp(-(1/2)(\underline{x}/v(\zeta))^2) \tag{2}$$

is a self-similar solution to the NLSE [25]

$$[i\partial_z + (1/2)\nabla_\perp^2 + |V(\underline{x}, \zeta)|^2]V(\underline{x}, \zeta) = 0. \tag{3}$$

The propagation problem is considered as the scalar one since a linear transverse electric (TE) polarization of the beam field V is assumed and all possible nonlinear changes of the beam polarization are neglected. In NLSE (3), a parabolic approximation of the field intensity term

$$|V(\underline{x}, \zeta)|^2 \simeq (1/2)w^{-2}(\zeta)(d(1 - \gamma(\zeta)) - (1 - \eta^2(\zeta))(\underline{x}/w(\zeta))^2) \tag{4}$$

in the sample refractive index distribution

$$n(\underline{x}, \zeta) = n_L + (1/2)n_2|E(\underline{x}, \zeta)|^2 = n_L(1 + (\beta z_D)^{-1}|V(\underline{x}, \zeta)|^2) \tag{5}$$

is presumed in the most general, *i.e.*, dependent on z, form [1]. In Equations (2)−(5), $A = a \exp(i\varphi)$ is a complex on-axis amplitude of the beam given by its magnitude a and phase φ; $v = (w^{-2} - iR^{-1})^{-1/2}$ is a complex beam radius (half-width) such as that $v = 1$ at $\zeta = 0$, $|V|^2$ stands for the normalized electric field intensity $|E|^2$,

i.e., $|V|^2 = (1/2)\beta z_D (n_2/n_L)|E|^2$, n_2 is the nonlinear refractive index, and $\nabla_\perp^2$ is the Laplace operator in the transverse coordinates. The spatial η and phase γ scale parameters are to be specified. It is assumed, however, that at low power levels the scale parameters are equal to one, which reduces the nonlinear problem to that of the linear propagation.

Within the SCRT method the nonlinear propagation problem can be transposed into the scaled linear propagation problem (indicated by the upper bar). The linear problem is governed by the paraxial reduced wave Fock equation [4]

$$[i\partial_{\bar{z}} + (1/2)\underline{\nabla}_\perp^2]\bar{V}(\underline{x}, \bar{z}) = 0, \tag{6}$$

with a well-known fundamental Gaussian solution [4], [5], [23]:

$$\bar{V}(\underline{x}, \bar{z}) = \bar{A}(\bar{z})\exp(-(1/2)(\underline{x}/\bar{v}(\bar{z}))^2), \tag{7a}$$

$$\bar{v}^2(\bar{z}) = \bar{v}^2(\bar{z}_0)(1 + i\bar{z})/(1 + i\bar{z}_0), \tag{7b}$$

$$\bar{A}(\bar{z}) = \bar{A}_0(\bar{v}(\bar{z}_0)/\bar{v}(\bar{z}))^d \tag{7c}$$

where at the input plane $z = z_0 = \bar{z}_0$ the beam complex amplitude $\bar{A} = \bar{a}\exp(i\bar{\varphi})$ and half-width $\bar{v} = (\bar{w}^{-2} - i\bar{R}^{-1})^{-1/2}$ are given by their unscaled counterparts, that is $\bar{A}_0 = A_0$ and $\bar{v}_0 = v_0$, respectively. Hence the definitions (7a)−(7c) imply

$$\int_{-\infty}^{+\infty} |\bar{V}(\underline{x}, \bar{z})|^2 d\underline{x} = \int_{-\infty}^{+\infty} |V(\underline{x}, \zeta)|^2 d\underline{x} = \pi^{d/2}(w_{wL}w_0)^d a_0^2. \tag{7d}$$

Equations (6), (7) constitute a convenient basis for the tracing of the nonlinear propagation process, provided that an appropriate transformation is available between the nonlinear problem ((2), (3)) and the scaled linear problem ((6), (7)).

The nonlinear-linear transformation is accomplished by introduction of two, dependent on ζ or z, scale parameters η and γ (*cf.* [1]), and subsequently, by a scale transformation of the optical path

$$\bar{z} - \bar{z}_0 = \eta(\zeta)(z - z_0), \tag{8}$$

the radius of the phase front curvature

$$\bar{R}(\bar{z}) = \eta(\zeta)R(\zeta), \tag{9a}$$

and the on-axis beam phase

$$\bar{\varphi}(\bar{z}) - \bar{\varphi}_0 = (\eta(\zeta)/\gamma(\zeta))(\varphi(\zeta) - \varphi_0). \tag{10a}$$

Under the scaling transformation (8)−(10) the (real) beam half-width w and amplitude a remain unchanged. Thus, the inverse of the beam complex radius squared $v^{-2} = w^{-2} - iR^{-1}$ and the beam on-axis complex amplitude $A = a\exp(i\varphi)$ are also transformed by the transformation (8)−(10) to their respective scaled counterparts:

$$\bar{v}^{-2}(\bar{z}) = w^{-2}(\zeta) - i\eta^{-1}(\zeta)R^{-1}(\zeta), \tag{9b}$$

$$\bar{A}(\bar{z}) = a(\zeta)\exp(i\varphi_0)\exp[i(\eta(\zeta)/\gamma(\zeta))(\varphi(\zeta) - \varphi_0)]. \tag{10b}$$

As a result of the transformation ((8)−(10)), the linear scaled solution (7) uniquely determines the nonlinear unscaled solution ((1), (2)) to NLSE ((3), (4)) in each sufficiently thin section (from z_0 to z) of the nonlinear sample [1]. In order to solve the problem of the beam nonlinear propagation in the nonlinear sample, it is now sufficient to apply the scale transformation at the front (input or entry) face of the sample $z = z_0$, to trace the nonlinear propagation on the scaled linear level, and to apply the transformation inverse to (8)−(10) at the rear (output or exit) face, or at the arbitrary internal transverse plane of the sample. A schematic of such a solution construction is depicted in Fig. 1.

The solution obtained ((1), (2), (6)−(10)) remains only formal as far as the scale parameters are not explicitly specified. However, the scale parameters can be uniquely determined [1] by imposing on Eqs. (1)−(5) the constraints that make the solution ((1), (2), (7)−(10)) equivalent to the reduced variational solution of the propagation problem [24], [25]. According to this procedure (cf. [1]), the scale parameters are given by

$$\eta^2(\zeta) = 1 - (P/P_c)(w(\zeta)/w_0)^{-d+2}, \tag{11}$$

$$\gamma(\zeta) = 1 - (2/d)(1+d/4)(P/P_c)(w(\zeta)/w_0)^{-d+2} \tag{12}$$

and they are determined by the beam-power level [1]

$$P/P_c = a_0^2 w_0^2 / 2^{d/2}, \tag{13a}$$

which, in turn, is determined by the input beam on-axis amplitude a_0 and beam radius w_0 at the input plane $\zeta = \zeta_0$. The beam amplitude a_0 equals $2^{d/4}$ and the beam half-width w_0 equals one for $P/P_c = 1$ and $R^{-1} = 0$, i.e., for the self-trapped reduced variational solution to the NLSE ((3), (4)), [1], [24], [25]. Thus $(a_0 w_0)^2 = 2^{d/2}$ for $P/P_c = 1$ and $R^{-1} = 0$, and the power level P/P_c is a dimensionless measure of the beam power with respect to its counterpart in the self-trapped propagation. It must be also recalled that the case $P/P_c = 1$ indicates the self-trapped variational solution only for a perfectly collimated input beam, i.e., for $R_0^{-1} = 0$.

The ratio P/P_c can be alternatively given by the propagation power parameter

$$P = \pi^{d/2} w_{wL}^d 2^{-1} Y_L |E(0,0)|^2 = \pi^{d/2}(w_{wL} w_0)^d (\beta z_D)^{-1} Y_L (n_L/n_2) a_0^2, \tag{13b}$$

expressed by the on-axis intensity of the beam field at the waist $|E(0,0)|^2$ and scaled by the self-trapped propagation power parameter

$$P_c = (2\pi)^{d/2} \beta^{-2} w_{wL}^{d-2} Y_L (n_L/n_2) \tag{13c}$$

where Y_L is a characteristic low power admittance of the nonlinear medium. For the self-trapped propagation power level $P = P_c$, $\eta = 0$, $\gamma = 1 - (2/d)(1+d/4)$ [1]. Above this level, the scale parameter η becomes purely imaginary, but the field expressions (1)−(12) still remain valid.

It is pertinent to note that P_c denotes a self-trapped soliton power density (in watts/meter − due to a planar geometry) for $d = 1$ (cf. [24]), a critical (self-trapped) power (in watts) for self-focusing for $d = 2$ (cf. [25]), and an integrated power, i.e., an energy (in joules), of a self-trapped light bullet for $d = 3$ (cf. [26]). In the general

case, that is for arbitrary value of d, the parameter P_c should be regarded as the integrated intensity of the self-trapped solution to the NLSE (*cf.* [25], [26]). As the parameter P_c refers to the self-trapped solution of the NLSE ((3), (4)) for arbitrary value of d, the name "the self-trapped propagation power parameter" attributed to P_c seems appropriate in the multidimensional analysis given in this paper. However, one should have in mind that this parameter denotes strictly the beam power only in the three-dimensional case, *i.e.*, for $d = 2$. Note also that the SCRT formalism does not depend on the expression of P_c by itself but only on the ratio P/P_c, and that this ratio is determined in Eq. (13a) only by two beam parameters a_0 and w_0, *i.e.*, independent of common factors in Eqs. (13b) and (13c).

With the specification ((11), (12)) of the scale parameters, and with real values of P/P_c, the SCRT method traces the nonlinear propagation in the focusing Kerr medium. However, the derivation of the solution (1), (2), (6)−(13) remains valid for negative values of n_2 as well, that is for beam propagation in the defocusing Kerr medium. The same regularity concerns the reduced variational analysis [24], [25], on which the specification of the scale parameters ((11), (12)) is based. The negative sign of n_2 implies, through the beam intensity normalization, that the magnitude of the beam complex amplitude a takes imaginary values and the beam field intensity $|V|^2$ becomes negative what is consistent, for example, with propagation of dark solitons in the defocusing Kerr medium for $d = 1$ [24]. Therefore, expressions (1), (2), (6)−(13) can directly be used for $n_2 < 0$, at least for beams of moderate power, by a simple continuation procedure of P_c (13c) from its positive values for the focusing medium to its negative values for the defocusing medium. In this way, the scale tracing method remains valid also for the defocusing nonlinearities at sufficiently low field intensities, such that the shape of the beam remains approximately fundamental Gaussian. Validity of this continuation procedure is also confirmed by independent analyses of nonlinear propagation in the focusing and defocusing media for $d = 2$ (*cf.* [15], [17], [20]), to which the presented analysis gives equivalent results (in the beam field intensity evaluation), for both cases $n_2 > 0$ and $n_2 < 0$ in the three-dimensional geometry, *i.e.*, for $d = 2$.

The nonlinear term in the NLSE

$$|V|(\underline{x}, \zeta)|^2 = (P/P_c)w^{-d}(\zeta)w_0^{d-2}(1 + d/4 - (1/2)(\underline{x}/w(\zeta))^2) \tag{14}$$

differs substantially from the common first-order approximation $\exp(-(x/w)^2$ $\simeq 1 - (x/w)^2$ assumed in the conventional aberrationless analysis [7], [16]. The presented specification of the scale parameters ((11), (12)) provides solution appropriately averaged [1], [24], [25] in each transverse cross-section of the beam, with a self-consistent evaluation of both beam amplitude and phase. As a result, the cases of the "thin" and "thick" samples [13] are here treated in the same unified manner, without a need to resort to any correction factor, necessary to make the conventional analysis more accurate [13], [15]. The linear tracing (8)−(13) of the nonlinear propagation by a straight complex ray can be applied directly to the nonlinear sample of arbitrary thickness for the (2+1)-geometry ($d = 2$), since the scale parameters η and γ prove to be constant for $d = 2$. In other cases ($d = 1$ or $d = 3$),

the appropriate segmentation of the "thick" sample into a sequence of consecutive "thin" slices should be applied first, before getting a final solution traced by a curved ray this time [1]. The "thin" sample problem is defined within a range of ζ in which the scale parameters are approximately constant, i.e., for $\eta \simeq \eta_0$, $\gamma \simeq \gamma_0$ [1]. In the next Section, it appears, however, that a final outcome of the SCRT analysis remains common in a form of solution, independent of the geometry of the problem considered.

3. Evolution of beam parameters

The nonlinear character of the propagation entails a redefinition (1) of the optical distance from its low power value z to its nonlinear counterpart ζ. There are also expected, however, other nonlinear changes, namely, in the complex radius of the beam

$$v^2(\zeta) = w_w^2(\zeta)(1+i\zeta) = (w^{-2}(\zeta) - iR^{-1}(\zeta))^{-1} \tag{15}$$

and in the on-axis complex amplitude of the beam

$$A(\zeta) = \alpha(\zeta)A_0(v_0/v(\zeta))^d, \tag{16}$$

as described by the nonlinear change w_w of the beam radius at the waist and the nonlinear change α of the beam complex amplitude. Note that under the normalization imposed in Section 2 the low power beam radius w_L at the waist is equal to one, i.e., $w_L = 1$ at $z = 0$. In Eq. (15) the (real) beam radius $w = w_w(1+\zeta^2)^{1/2}$ and the radius of phase front curvature $R = w^2/\zeta$ are given consistently with the common low power definition of the complex width [4], [5], [23]. Therefore, the self-similar form of the solution (2) to the NLSE (3) is given in a well-known form of the linear propagation [4], [5], [23], as far as one disregards the nonlinear changes in the optical distance, in the actual position of the beam waist, in the beam waist width and in the beam complex amplitude. These changes, referred to as the nonlinear aberrationless effects, are given by the following nonlinear aberrationless parameters: the self-shortening factor $\varkappa$, the shift of the beam waist δ_z, the beam waist width modification w_w and the complex amplitude modification α, respectively. A solution introduced in Section 2 provides a specification of these parameters. Let us restate the solution (1), (2), (6)−(13) in a form suitable to the evaluation of these parameters.

The solution to the scaled linear propagation (7), together with the scale transformation (8)−(10), yields the solution in the unscaled space in the semi-linear form (1), (2), (cf. also [1]). It can be described by two coupled first order ordinary differential equations for the evolution of the (real) beam parameters w and ζ:

$$(d/dz)(w^2(\zeta)\zeta^{-1}) = 1 - \eta^2(\zeta)\zeta^{-2}, \tag{17}$$

$$w(\zeta)(d/dz)(w(\zeta)) = \zeta. \tag{18}$$

In each sample slice thin enough to fulfil the condition $\eta = \eta_0$ [1], Eqs. (17), (18) have the solution in a form of the nonlinear changes of the beam radius

$$w^2(\zeta) = w_0^2((1+z_0 w_0^{-2}(z-z_0))^2 + \eta^2(w_0^{-2}(z-z_0))^2), \tag{19}$$

and of the nonlinear optical path increment

$$\zeta - \zeta_0 = \eta^2(1 + z_0^2/\eta^2)w_0^{-2}(z-z_0), \tag{20}$$

which yields the adequate nonlinear modifications of the beam waist radius w_w and the optical distance ζ. The nonlinear optical distance ζ, together with the actual beam waist position at $\zeta = 0$ as well, are uniquely determined by their nonlinear changes with respect to the low power optical distance z and specified by the initial conditions $a = a_0$ and $w = w_0$ at $z = z_0$. Note that, by analogy to the linear propagation, the radius of the beam phase curvature R is defined by w and ζ as $R = w^2/\zeta$. Note also that Eqs. (1), (17), (18) can be decoupled into the second order differential equation for the beam width

$$(d^2/dz^2)w(\zeta) = \eta^2(\zeta)w^{-3}(\zeta) \tag{21}$$

and the first order differential equation for the beam optical path

$$d\zeta/dz = \eta_0^2(1+\zeta_0^2/\eta(\zeta))/(1+\zeta_0^2), \tag{22}$$

and that Eq. (21) itself leads to the potential good description of the beam dynamic changes during the beam nonlinear propagation [1], [24], [25].

Apart from the nonlinear changes of the optical distance, expressions (15), (17)−(22) concern only the beam complex radius v. On the other hand, Eqs. (2), (7)−(10) determine also the complex amplitude A of the beam through the law of the beam power conservation

$$a^2(\zeta)w^4(\zeta) = a_0^2 w_0^4, \tag{23}$$

and the explicit changes of the on-axis phase of the beam

$$(d/dz)\varphi(\zeta) = -(d/2)\gamma(\zeta)w^{-2}(\zeta). \tag{24}$$

While relation (23) directly expresses the beam on-axis amplitude a, a solution to the on-axis phase equation is given by

$$\varphi(\zeta) - \varphi_0 = (\gamma(\zeta)/\eta(\zeta))(\varphi_L(\zeta/\eta(\zeta)) - \varphi_L(\zeta_0/\eta_0)) = \varphi_L(\zeta) - \varphi_{L0} + \delta_\varphi(\zeta) - \delta_{\varphi 0}, \tag{25a}$$

in each sample slice thin enough to fulfil condition $\eta \simeq \eta_0$, $\gamma = \gamma_0$ [1]. The on-axis phase modification effect δ_φ is to be given below, and

$$\varphi_L(\zeta/\eta) = \begin{cases} -(d/2)\arctan(\zeta/\eta), & \eta^2 > 0 \\ +(d/2)i\,\mathrm{arctanh}(\zeta/(-i\eta)), & \eta^2 < 0 \end{cases} \tag{26}$$

is expressed in Eqs. (25), (26) by the function $\varphi_L(z)$ characteristic of the low power on-axis phase. Note that, in general, the argument of the on-axis complex amplitude A is

$$\arg(A(\zeta)) = \arg(A_0) + \varphi(\zeta) - \varphi_0, \tag{25b}$$

that is, $\arg(A_0) = \varphi_0$ if and only if $\arg(A(0)) = 0$.

Finally, on the grounds of Eqs. (16), (23)−(25), the complex on-axis amplitude A and its nonlinear modification α are given by

$$A(\zeta) = A_0(w_0/w(\zeta))^{d/2}\exp(i(\varphi(\zeta)-\varphi_0)) = \alpha(\zeta)A_0(v_0/v(\zeta))^d, \tag{27}$$

$$\alpha(\zeta) = (w_w(\zeta)/w_{w0})^{d/2}\exp(i(\delta_\varphi(\zeta)-\delta_{\varphi0})) \tag{28}$$

where $w_{w0} = w_w(\zeta_0)$, etc. Equations (27), (28) have been derived within the thin sample approximation $\eta \simeq \eta_0$, $\gamma \simeq \gamma_0$ [1]. However, Eq. (28) implies that a form of solution (27), (28) remains unchanged also for the thick sample case due to the additive nature of the aberrationless changes of the beam phase and multiplicative nature of such changes of the beam (real) amplitude. This feature of the solution (27), (28) enforces the intermediate phase components and amplitude factors to be cancelled under consecutive applications of formulae (27), (28) in the solution construction for the thick sample, from subsequent solutions for thin slices of this sample. Hence, expression (28) for the aberrationless effect in the beam complex amplitude remains valid in the arbitrary configuration, i.e., for arbitrary sample thickness L and a number of the transverse dimensions d.

4. Spatial and phase aberrationless effects

On the grounds of Equation (20), expression (1) for the optical path can be restated as

$$\zeta = \varkappa(z-\delta_z) \tag{29}$$

where $\varkappa$ stands for the nonlinear self-shortening factor

$$\varkappa = \eta_0^2(1+\zeta_0^2/\eta_0^2)/(1+\zeta_0^2) \tag{30}$$

and δ_z denotes the nonlinear waist shift

$$\delta_z = \zeta_0(1-\varkappa^{-1}) = \zeta_0(1-\eta_0^{-2})/(1+\zeta_0^2/\eta_0^2) \tag{31}$$

where η_0 stands for initial value of η. In a thin sample case $\eta = \eta_0$ or for $d = 2$ both quantities $\varkappa$ and δ_z are constant for a given beam power level P/P_c and explicitly specified by the initial field parameters w_0, R_0 and a_0. In the opposite case, namely in thick samples and for $d = 1$ or $d = 3$, the quantities $\varkappa$ and δ_z vary with ζ. But still, this variation is small as $\varkappa$ and δ_z depend on ζ only through the function $\eta(\zeta)$. From Eqs. (19), (20) the beam waist radius w_w or the nonlinear beam waist modification takes a form

$$w_w^2(\zeta) = ((1+\zeta_0^2)/(1+\zeta^2))((1+\zeta^2/\eta^2(\zeta))/(1+\zeta_0^2/\eta_0^2)). \tag{32}$$

Note that $w_w/w_{wL} = w_w$, as $w_{wL} = 1$ for the low power propagation. Moreover, from Eqs. (25)−(28) it can be shown that the phase of the beam

$$\varphi(\zeta) = \varphi_L(\zeta) + \delta_\varphi(\zeta) - \delta_{\varphi0} \tag{33}$$

is nonlinearly modified by the nonlinear on-axis phase shift component

$$\delta_\varphi(\zeta) = (\gamma(\zeta)/\eta(\zeta))\varphi_L(\zeta/\eta(\zeta)) - \varphi_L(\zeta) \tag{34}$$

where $\delta_{\varphi 0} = \delta_\varphi(\zeta_0)$. Both nonlinear effects w_w and δ_φ depend directly on ζ, in all cases of $d = 1, 2, 3$, and their variation with ζ is much more pronounced than the ζ-variation of $\varkappa$ and δ.

Equations $(27)-(34)$ explicitly indicate that the paraxial Gaussian beam is completely described by the four independent aberrationless effects: the self-shortening factor $\varkappa$ (30), the waist shift δ_z (31), the waist radius modification w_w (32), and the nonlinear on-axis phase shift $\delta_\varphi - \delta_{\varphi 0}$ (33), (34). The last two effects w_w and $\delta_\varphi - \delta_{\varphi 0}$ show significant variation along the nonlinear propagation optical distance ζ. The nonlinear change α of the complex amplitude of the beam, as given by Eq. (28), is expressed by the aberrationless parameters w_w and $\delta_\varphi - \delta_{\varphi 0}$ and, therefore, cannot be regarded as the independent aberrationless effect. However, Eqs. (27), (28) indicate that both on-axis (real) amplitude and phase of the beam undergo changes during nonlinear propagation, as compared to their counterparts evaluated for the low power propagation case. The changes of the beam parameters are exemplified in Figs. $2-4$.
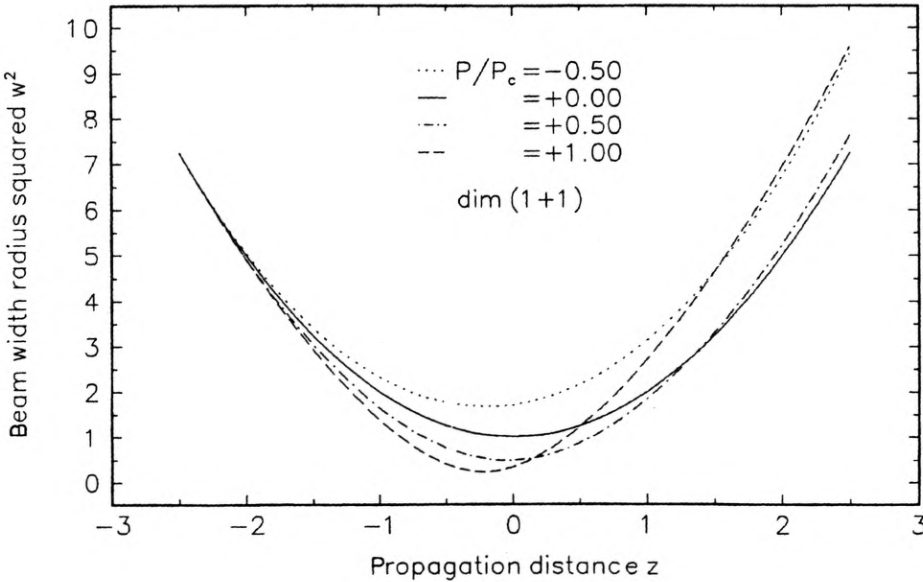

Fig. 2. Beam width radius squared w^2 versus the low power propagation path z, as measured for different beam power levels P/P_c; $L/n_L = 5.0$, $\Delta_z = 0.0$, dim $(1+1)$

The nonlinear change of the beam width radius along the propagation in the nonlinear sample is shown in Fig. 2 in the planar dim $(1+1)$ configuration. These changes depend not only on the medium nonlinearity or the beam power but also on the incident beam convergence. The (nonzero) beam convergence is determined by a central position of the low power waist, *i.e.*, for the low power waist offset $\Delta_z = 0$ from the centre (symmetry) plane of the sample. The waist width decreases with the
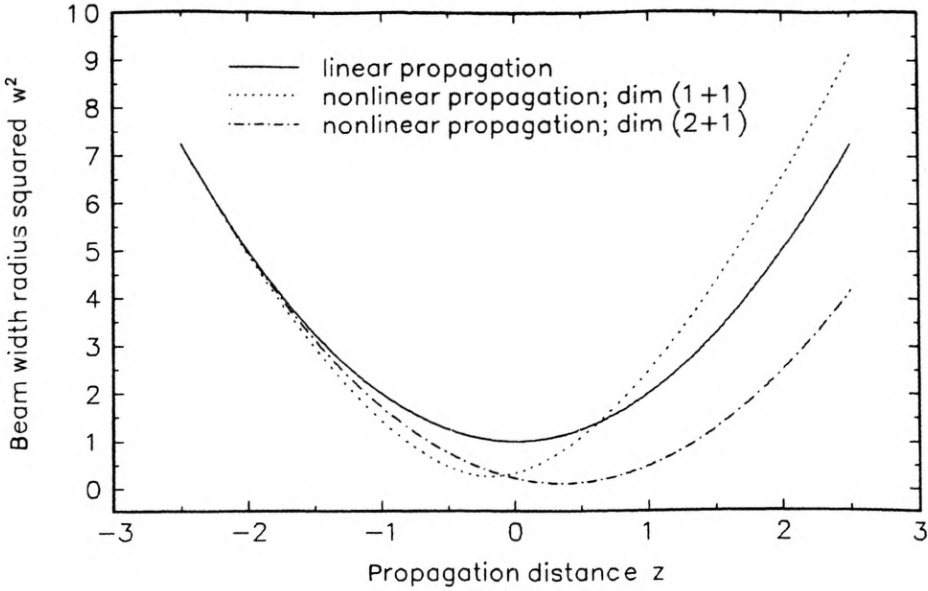
Fig. 3. Beam width radius squared w^2 versus the low power propagation path z, as measured for different geometries dim $(1+1)$ and dim $(2+1)$; $P/P_c = 0.9$, $L/n_L = 5.0$, $\Delta_s = 0.0$. Linear changes of the beam radius are shown for comparison
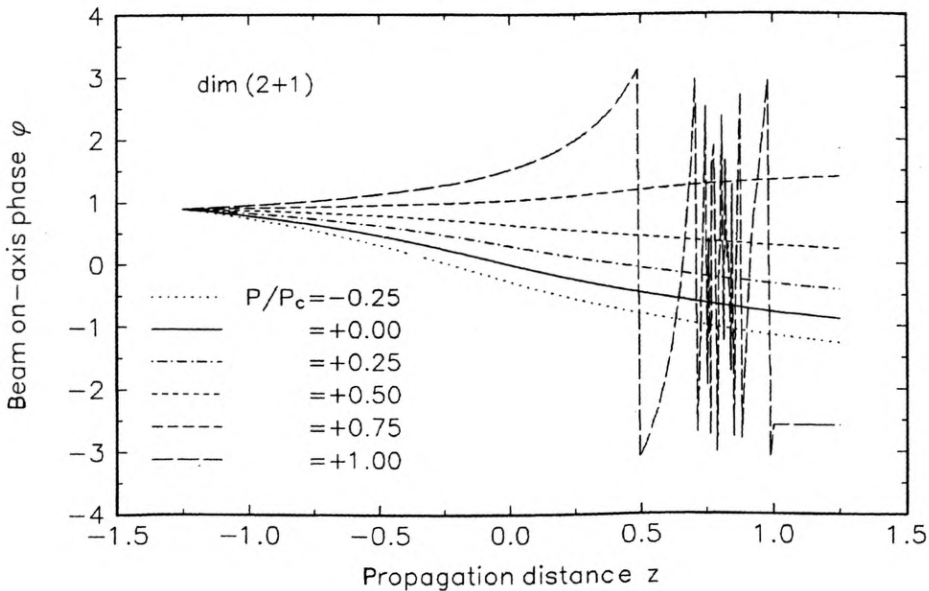

Fig. 4. Total on-axis phase of the beam versus the low power propagation path z, as measured for different beam power levels P/P_c; $L/n_L = 2.5$, $\Delta_s = 0.0$, dim $(2+1)$

beam power increase, as expected. Moreover, the waist shift increases (to the right from the sample centre) with the increasing power. However, these changes are not monotone for high beam powers. It appears that near the self-trapped power level and in specified regions of the nonlinear sample, a direction of these changes of the beam width can be reversed (*cf.* Fig. 2, curves $P/P_c = 0.5$, 0.1). Note that such situation occurs only for highly convergent beams and sufficiently thick nonlinear samples in the planar geometry, contrary to the case dim $(2+1)$, in which all changes show a clear monotone character. Note also that, due to the nonzero phase front curvature at the input plane, the beam radius varies even at the power level $P/P_c = 1$.

The differences between the two-dimensional (dim $(1+1)$) and three-dimensional (dim $(2+1)$) propagation cases are especially pronounced in thick nonlinear samples. Such a situation is shown in Fig. 3, where the nonlinear changes of the beam radius are compared with the adequate linear (low power) changes for the sample thickness five times larger than the propagation distance z_D and for the low power beam waist placed in the centre of the sample, *i.e.*, $\Delta_z = 0$. The high convergence of the incident beam results in reversing sign of the waist shift (to the left from the sample centre) and in reversing sign of the beam radius aberrationless modification in configuration dim $(1+1)$, as compared to the prediction in dim $(2+1)$ geometry (here for $z > 0$). Therefore, Fig. 3 directly confirms that the aberrationless effects qualitatively depend on the number d of the transverse dimensions of the propagation problem considered.

Figure 4 displays the total on-axis phase of the beam, as modified by the aberrationless on-axis phase modification for the case dim $(2+1)$. This modification becomes stronger for higher beam powers and above the power level $P/P_c = 2/3$ the phase changes reverse their sign. Significance of this fact in optical pulse compression by spatio-temporal coupling of the self-focusing and phase self-modulation has been discussed recently [22], [25], [27], [28]. For the self-trapping level $P/P_c = 1$ the beam approaches its self-collapse point at $z = 0.8$. Near the self-collapse point the beam phase suffers from rapid changes. Beyond this point, however, the nonlinear on-axis phase modification cancels exactly the low power phase changes and gives rise to a constant on-axis phase of the beam, as can be seen at the right-bottom part of Fig. 4.

The most significant feature of the aberrationless nonlinear effects is their direct geometrical interpretation. They should appear particularly useful in analysis of the nonlinear phenomena, where a nonlinear process depends primarily on geometrical parameters of the propagating beam. As an example, the configurations should be indicated, in which the optical beam interacts with a diaphragm placed inside an optical system, as it takes place in the Z-scan measurements of the nonlinear medium parameters [13], [18], [19], [29] or Additive-Pulse and Kerr-Lens Mode Locking phenomena in lasers cavities [8], [14], [15], [20], [21]. Another pertinent example is a spatio-temporal coupling encountered during nonlinear propagation and leading to the nonlinear pulse compression [22], [27], [28]. In general, the SCRT method, and its semi-linear aberrationless version in particular, should potentially find

applications in theory of nonlinear optics, because of the simple linear form of the final equations.

5. Higher-order mode propagation

It is evident that using the fundamental Gaussian Ansatz one can model the nonlinear propagation only for a limited range of the beam power. Therefore, it would be profitable to extend the SCRT method into the case of the higher-order Hermite−Gaussian functions [4], [5], [30]−[34]. Moreover, it seems possible, per analogy to the extensions used in analysis of the linear propagation phenomena [4], [5] to use the Hermite−Gaussian beam in a symmetric form in arguments of the exponent and Hermite functions [1]

$$V_n(\underline{x},\zeta) = A_n(\zeta)\exp(-(1/2)(\underline{x}/v)(\zeta))^2)\prod_{j=1}^{d} H_n(2^{-1/2}x_j/v_n(\zeta)) \tag{35}$$

where the Hermite polynomials H_n

$$H_n(y) = (-1)^n\exp(y^2)(d^n/dy)^n\exp(-y^2) \tag{36}$$

satisfy the second-order ordinary differential equation

$$H_n'' - 2^{1/2}(x_j/v_n(\zeta))H_n' + 2nH_n = 0. \tag{37}$$

In Equation (37), the prime denotes a differentiation with respect to the argument of H_n and the subscript $n = 2l$, $l = 0,1,2$, indicates the Hermite−Gaussian function of even order. Such version of the Hermite−Gaussian function was introduced by SIEGMAN [30] and their relevance has been firmly confirmed, *e.g.*, in the problem of Gaussian beam interaction with planar dielectric interfaces [5], [33]. Substitution the parabolic approximation of the field intensity (*cf.* [1])

$$|V(\underline{x},\zeta)|^2 \simeq c(\zeta) - b(\zeta)\underline{x}^2 \tag{38}$$

into NLSE (3) leads to the independent equation for the complex radius v_j of each Hermite polynomial

$$iv^{-4}(\zeta)[(d/dz)(v^2(\zeta)) - i] - 2b(\zeta) = 0, \tag{39}$$

the appropriately modified complex amplitude equation

$$2i(d/dz)(\ln A_n(\zeta)) - d(nv_n^{-2}(\zeta) + v^{-2}(\zeta)) + 2c(\zeta) = 0, \tag{40}$$

and the compatibility relation

$$iv_n^{-2}(\zeta)[v_n^{-2}(\zeta)(d/dz)(v_n^2(\zeta)) - i(2v^{-2}(\zeta) - v_n^{-2}(\zeta))] = 0, \tag{41}$$

between the higher-order and fundamental complex half-widths v_n and v, respectively. The complex ray equation (39) appears common to the Hermite−Gaussian function of any (even) order. Moreover, in the fundamental mode case $n = 0$, the compatibility condition (41) reduces to the ray equation (39). For the

higher-order case all three independent equations (39)−(41) are necessary to describe the ray tracing of the propagation process.

A separate matter is how to specify the scale parameters in Eqs. (38)−(41). In the fundamental propagation case, the application of the scale transformation (8)−(10) leads to the scale parameters evaluation given by Eqs. (11)−(13). In the general even higher-order mode propagation case, the widths v_n and v must be different to avoid the contradiction between the complex ray equation (39) and the compatibility condition (41). Therefore, in order to determine the scale parameters for the higher-order propagation, the conventional variational analysis [24], [25] should be first considerably modified accordingly to the ray equation (39), transport equation (40) and compatibility condition (41), or other equivalent procedure should be invented instead. That points out a direction of further research on the extensions of the SCRT method.

6. Conclusions

The semi-linear aberrationless paraxial approach to the nonlinear propagation in Kerr media has been presented. Basic features of the SCRT method have been summarized and a self-consistent set of equations for beam parameters evolution have been explicitly given. It has been shown that the nonlinear process can be completely described in terms of four aberrationless nonlinear effects: the optical distance self-shortening, the beam waist nonlinear shift, the beam waist width modification and the on-axis phase shift. The generalization of the SCRT method into the higher-order mode nonlinear propagation has been outlined. The numerical simulations, as enclosed here and to be published in an accompanied paper [34], indicate usefulness of the description of the nonlinear propagation in terms of the aberrationless nonlinear effects.

References

[1] NASALSKI W., Opt. Appl. 24 (1994), 205; Opt. Commun. 119 (1995), 218.
[2] LAX M., LOUISELL W. H., MCKNIGHT W. B., Phys. Rev. A 11 (1975), 1365.
[3] NAZARATHY M., SHAMIR J., J. Opt. Soc. Am. 72 (1982), 1398.
[4] SIEGMAN A. E., *Lasers*, Univ. Sci. Books, Mill Valley 1986, pp. 581−922; ARNAUD J. A., *Beam and Fiber Optics*, Academic Press, New York 1976.
[5] NASALSKI W., IFTR Reports 32 (1990), 1−152, Habilitation Thesis (in Polish).
[6] TREACY E. B., IEEE J. Quantum Electron. 5 (1969), 454; DIJAILI S. P., DIENES A., SMITH J. S., IEEE J. Quantum Electron. 26 (1990), 1158.
[7] AKHMANOV S. A., KHOKHLOV R. V., SUKHORUKOV A. P., [In:] *Laser Handbook*, [Eds.:] F. T. Arecchi, E. O. Schulz-Dubois, North-Holland, Amsterdam 1972, Vol. 2, Chapt. E3, 1151; MARBURGER J. H., Prog. Quantum Electron. 4 (1975), 35.
[8] HERMANN J. A., J. Modern Opt. 35 (1988), 1777.
[9] SNYDER A. W., MITCHELL D. J., POLADIAN L., J. Opt. Soc. Am. B 8 (1991), 1618.
[10] BÉLANGER P. A., PARÉ C., Appl. Opt. 22 (1983), 1293.

[11] GAGNON L., PARÉ C., J. Opt. Soc. Am. A **8** (1991), 601.

[12] GAGNON L., J. Opt. Soc. Am. B **7** (1990), 1098.

[13] SHEIK-BAHAE M., SAID A. A., HAGAN D. J., SOILEAU M. J., VAN STRYLAND W. W., Opt. Eng. **30** (1991), 1228.

[14] SALIN F., SQUIER J., PICHÉ M., Opt. Lett. **16** (1991), 1674.

[15] HUANG D., ULMAN M., ACIOLI L. H., HAUS H. A., FUJIMOTO J. G., Opt. Lett. **17** (1992), 511.

[16] GEORGIEV G., HERRMANN J., STAMM U., Opt. Commun. **92** (1992), 368.

[17] MAGNI V., CERULLO G., DE SILVESTRI S., Opt. Commun. **96** (1993), 348; ibidem **101** (1993), 365.

[18] SHEIK-BAHAE M., SAID A. A., WEI T. H., HAGAN D. J., VAN STRYLAND E. W., IEEE J. Quantum Electron. **26** (1990), 760.

[19] HERMANN J. A., MCDUFF R. G., J. Opt. Soc. Am. B **10** (1993), 2056; CHAPPLE P. B., STARO-MLYNSKA J., MCDUFF R. G., J. Opt. Soc. Am. B **11** (1994), 975.

[20] HAUSS H. A., FUJIMOTO J. G., IPPEN E. P., IEEE J. Quantum Electron. **28** (1992), 2086.

[21] BRABEC T., SPIELMANN C., CURLEY P. F., KRAUSZ F., Opt. Lett. **17** (1992), 1292; BRABEC T., CURLEY P. E., SPIELMANN C., WINTER E., SCHMIDT A. J., J. Opt. Soc. Am. B **10** (1993), 1029.

[22] KARLSSON M., ANDERSON D., DESAIX M., LISAK M., Opt. Lett. **16** (1991), 1373.

[23] NASALSKI W., Opt. Commun. **77** (1990), 443; ibidem **92** (1992), 307; J. Opt. Soc. Am. A **13** (1996), 172.

[24] ANDERSON D., Phys. Rev. A **27** (1983), 3135.

[25] DESAIX M., ANDERSON D., LISAK M., J. Opt. Soc. Am. B **8** (1991), 2082.

[26] SILBERBERG Y., Opt. Lett. **15** (1990), 1282.

[27] MONASSAH J. T., GROSS B., Opt. Lett. **17** (1992), 976.

[28] RYAN A. T., AGRAVAL G. P., Opt. Lett. **20** (1995), 306.

[29] XIA T., HAGAN D. J., SHEIK-BAHAE M., VAN STRYLAND E. W., Opt. Lett. **19** (1994), 317.

[30] SIEGMAN A. E., J. Opt. Soc. Am. **63** (1973), 1093.

[31] PRATESI R., RONCHI L., J. Opt. Soc. Am. **67** (1977), 1274.

[32] WÜSHE A., J. Opt. Soc. Am. A **6** (1989), 1320.

[33] ANTAR Y. M. M., BOERNER W. M., IEEE Trans. Antenn. Propag. **22** (1974), 837.

[34] NASALSKI W., *Aberrationless effects of nonlinear propagation*, J. Opt. Soc. Am. B, to be published